Thermomechanics of the Variation of Interfaces in Heterogeneous Lyophobic Systems

Loïc Coiffard and Valentin A. Eroshenko
Ecole Polytechnique, X-Technologies, Laboratoire d'Energétique Thermomoléculaire, 91128 Palaiseau, France

Jean-Pierre E. Grolier
Laboratoire de Thermodynamique des Solutions et des Polymères, Université Blaise Pascal, 63177 Aubière, France

DOI 10.1002/aic.10371
Published online March 1, 2005 in Wiley InterScience (www.interscience.wiley.com).

A comprehensive investigation aimed at elucidating thermodynamic and mechanical behavior of heterogeneous systems, featuring an association of solid hydrophobic matrices (micro- or mesoporous) and water, has been undertaken. Scanning transitiometry techniques were applied for measurements of mechanical work and heat effects during cycles of isothermal compression/decompression. The interface variation during forced intrusion of water into the matrix porous space and its spontaneous expulsion show complicated thermal behavior patterns. Typical exothermic intrusion and expulsion are confirmed for certain categories of systems, whereas for others strong endothermic intrusion is detected. A simple thermodynamic model involving variable irreversibility in the liquid flow and in the contact line movement is proposed to explain such an original thermomechanical behavior. Consequences for mechanical devices based on these heterogeneous systems are fully discussed. © 2005 American Institute of Chemical Engineers *AIChE J,* 51: 1246–1257, 2005

Keywords: porous media, nonwetting, microcalorimetry, surface chemistry/physics, dissipative phenomena

Introduction

Solid–liquid interfaces can be used to generate and utilize surface energy taking advantage of molecular interactions in heterogeneous lyophobic systems. They can act as working bodies[1-4] to store,[5,6] release,[7] or transform[8,9] mechanical energy. For instance, the thermomechanical behavior of some hydrophobic grafted silica-gel in association with water has been harnessed to build efficient innovative dampers.[10,11] Others systems can work as "all-or-nothing" springs[12] or can be used as thermal machines in appropriate thermodynamic cycles.[13] The development of such mechanical devices is still in progress but one can reasonably expect improvements in efficiency, compactness, self-functioning, and compliance with environmental regulations. However, the design and the industrial realization of operating devices requires further insight into thermomechanical characteristics of these systems. In particular, in the case of a mechanical system such as a damper, to optimize its operation in terms of time and temperature it is essential to establish the thermal behavior during operation of the device. Previous hypothetic, mostly theoretical, views suggest an endothermic phenomenon associated with an increase of the nonwetting interface area under isothermal conditions. Under adiabatic isobaric conditions, this effect would cool the system.[14] Similarly, any decrease of the nonwetting interface area under isothermal conditions should be accompanied by an exothermic phenomenon.

However, recent calorimetric measurements on mesoporous hydrophobic-functionalized silica-gel–water systems suggest that increasing and decreasing the area of the nonwetting

Correspondence concerning this article should be addressed to L. Coiffard at loic.coiffard@polytechnique.fr.

interface are both accompanied by heat production under isothermal conditions.[15,16] More recent theoretical considerations and experimental studies[17,18] have demonstrated that the heat effect measured during an increase of the nonwetting interface area may actually vary from exothermic to endothermic, depending on the nature of the system and on the compression stage.[19]

The present work is devoted to evaluation and quantification of the exo- and endothermic effects produced in some heterogeneous systems during isothermal cycles of compression/decompression. Understanding the thermal behavior of such systems should contribute to a better understanding of the repulsive forces between a hydrophobic porous structure and a nonwetting liquid and therefore allow the design of effective operating devices.

Principles

In what follows energy added to the system is positive, whereas energy produced by the system is negative. Typically, the systems are composed of a porous solid, actually a powder that can develop a high inner specific surface, and of a liquid that is nonwetting, that is, that does not invade the porous volume of the solid at ambient pressure. Such an association exhibits a novel mechanical and thermal behavior.[3] Consisting of two condensed components, the system is very weakly compressible, and a change in volume is always associated with a large increase of pressure. However, at the pressure of intrusion (P_{int}), the liquid begins to penetrate the pores volume of the solid phase. P_{int} is given by the Laplace–Washburn equation

$$P_{int} \approx -\frac{2\sigma \cos \theta_A}{r} \tag{1}$$

If the repulsion of the two phases is great enough, the liquid phase will be expelled at a pressure P_{exp}, given by the following equation

$$P_{exp} \approx -\frac{2\sigma \cos \theta_R}{r} \tag{2}$$

In Equations 1 and 2 the residual pressure in pores is neglected compared to P_{int} and P_{exp}.[11] θ_A and θ_R are the dynamic contact angles (A for advancing, R for receding) for intrusion and expulsion, respectively. The minus sign in both equations comes from the value of the contact angle, which is $>90°$ for lyophobic surfaces, the corresponding cosine being negative. σ is the superficial tension of the liquid and r is the pore radius.

For a narrow pore-size distribution, the intrusion takes place over a narrow pressure range in which the system becomes highly compressible. Upon completion of intrusion the system returns to a state of low compressibility. Decompression of the system may show a spontaneous expulsion of the liquid from the pores over a narrow range of pressure of expulsion. The difference between the intrusion and expulsion pressures is characteristic of a hysteresis phenomenon, which can be expressed as

$$H = (P_{int} - P_{exp})/P_{int} \tag{3}$$

Systems that transform reversibly ($H = 0$) to completely irreversibly ($H = 1$), when no expulsion occurs, can be obtained.

The variation of internal energy dU during compression and decompression can be divided into two parts (Eq. 4): the variation arising from the volume change (superscript V) of the bulk liquid and solid (taken separately and neglecting the heterogeneous interface) and the variation of the interface area (superscript Ω) resulting from the change (increase or decrease) of the area of surface contact Ω between the liquid and solid phases. The last term appears only during intrusion and expulsion

$$dU = dU^V + dU^\Omega \tag{4}$$

The dU^V term can be expressed through the first principle of thermodynamics as the sum of work W and heat Q:

$$dU^V = \delta W^V + \delta Q^V \tag{5}$$

For isothermal conditions, the compressibility and the appropriate Maxwell relation, in the case of a homogeneous phase, can be expressed as

$$dV = -V\kappa_T dP \tag{6}$$

$$dS = -\alpha_P dP \tag{7}$$

In a heterogeneous system made of a liquid L and a porous solid M, when the liquid is outside of the porous solid, the changes in W and Q, for an isothermal, reversible change in pressure, can be expressed as

$$\delta W^V = -PdV^V = P(V^L\kappa_T^L + V^M\kappa_T^M)dP \tag{8}$$

$$\delta Q^V = TdS^V = -T(V^L\alpha_P^L + V^M\alpha_P^M)dP \tag{9}$$

where κ_T and α_P are the isothermal compressibility and isobaric expansivity respectively for the liquid (superscript L) and the solid (superscript M). Thus, in principle, an isothermal compression will produce heat, whereas an isothermal decompression will absorb heat. It is not certain that Eqs. 6 and 7 remain valid if the liquid is inside the porous volume. The physical properties of the solid may change between the beginning of the intrusion (stress is applied only externally on the porous structure) and after completion of the intrusion (stress is applied both on internal and external solid surfaces). The physical properties of the liquid in the confined state may also change. After completion of the intrusion, corrected thermodynamic coefficients should be used in Eqs. 8 and 9, although such correction will not be considered in what follows.

The contribution to the change in internal energy from the change in the surface area of contact can be expressed as

$$dU^\Omega = \delta W^\Omega + \delta Q^\Omega \tag{10}$$

Work exchanged during intrusion and expulsion can be written for a two- (2D) or a three-dimensional (3D) process, respectively, as

$$W_{int}^{\Omega} = \int P_{int} dV_{inv} \qquad \text{or} \qquad W_{int}^{\Omega} = -\int \sigma \cos\,\theta_A d\Omega_{inv} \tag{11}$$

and

$$W_{exp}^{\Omega} = \int P_{exp} dV_{inv} \qquad \text{or} \qquad W_{exp}^{\Omega} = -\int \sigma \cos\,\theta_R d\Omega_{inv} \tag{12}$$

where V_{inv} is the porous volume of the matrix occupied by the liquid (dV_{inv} is positive for intrusion and negative for expulsion) and Ω_{inv} is the specific surface of the solid–liquid interface ($d\Omega_{inv}$, reduced to $d\Omega$ in what follows, positive for intrusion and negative for expulsion). During intrusion a certain amount of energy from work is stored in the system. The larger the pressure of intrusion or the porous volume, the larger the stored energy. During expulsion a certain amount of energy is released, always smaller than the amount of work previously done on the system ($90° < \theta_R < \theta_A$).

Previous theoretical studies on isothermal intrusion and expulsion of a nonwetting liquid into or from a porous matrix have dealt solely with the case of a reversible process.[14] In that case, one can assume the existence of a static contact angle and define the reversible work during an interfacial surface variation $d\Omega$ as

$$\delta W_{rev}^{\Omega} = -\sigma \cos\,\theta_{St} d\Omega \tag{13}$$

Concerning the entropy variation, without any assumption and for isothermal conditions, one can obtain

$$dS_{rev}^{\Omega} = \frac{d(\sigma \cos\,\theta_{St})}{dT} d\Omega \tag{14}$$

and thus for the heat exchanged,

$$\delta Q_{rev}^{\Omega} = T\left(\frac{d\sigma}{dT} \cos\,\theta_{St} - \sigma \frac{d\theta_{St}}{dT} \sin\,\theta_{St}\right) d\Omega \tag{15}$$

Both the surface tension and the static contact angle can be temperature dependent and the second term of Eq. 15 is not a priori negligible compared to the first term.[13] Investigation of the temperature dependency of the contact angle is still in progress; however, when the contact angle is much larger than 90° it appears to be temperature independent. A very weak decrease of the contact angle is observed over a large temperature range. Given that $d\sigma/dT$ has a minus sign for practically all liquids, both terms of Eq. 15 have the same sign and contribute to the heat effect in the same way. Taking the sine of the contact angle reduces the influence of the second term on the value of δQ_{rev}^{Ω}, and as a first assumption, Eq. 15 can be rewritten as

$$\delta Q_{rev}^{\Omega} \approx T \frac{d\sigma}{dT} \cos\,\theta_{St} d\Omega \tag{16}$$

Equations 13–16 are valid during reversible intrusion and expulsion in an isothermal transformation. Equation 16 postulates that intrusion, which increases the surface of contact between the solid and the liquid $d\Omega > 0$, causes an endothermic effect ($\delta Q_{rev}^{\Omega} > 0$), whereas expulsion ($d\Omega < 0$) causes an exothermic effect ($\delta Q_{rev}^{\Omega} < 0$) of equal absolute value. As a matter of fact, intrusion generates two energetic storages,[14] mechanical and thermal, that have identical absolute values (qualitatively and quantitatively) to those generated during expulsion.

In an irreversible process at constant T the irreversibilities degrade work into heat and thus create entropy in the surroundings. The work and heat resulting from the change in the surface contact can be divided into two terms

$$\delta W^{\Omega} = \delta W_{rev}^{\Omega} + \delta W_{irr} \tag{17}$$

$$\delta Q^{\Omega} = \delta Q_{rev}^{\Omega} + \delta Q_{irr} \tag{18}$$

where the entropy created δS_c comes as

$$\delta W_{irr} = -\delta Q_{irr} = T\delta S_c \tag{19}$$

Evidently, even if the absolute values of δW_{rev}^{Ω} and δQ_{rev}^{Ω} do not depend on the direction (intrusion or expulsion), the values of δW_{irr} and δQ_{irr} may differ between intrusion and expulsion because the two modes may be different, that is, a forced intrusion and a spontaneous expulsion ($\delta W_{irr,int} \neq \delta W_{irr,exp}$ and $\delta Q_{irr,int} \neq \delta Q_{irr,exp}$). The above equations apply differently between the intrusion and the expulsion processes because part of the work done on the system during intrusion is degraded into heat and part of the heat produced during expulsion arises from the degradation of mechanical energy.

During intrusion and expulsion we have a twofold heat effect.[18] First, there is an endothermic effect during intrusion that becomes exothermic during expulsion. This effect is directly proportional to the area of the interface. Second, there is an exothermic effect during the intrusion that is also exothermic during expulsion. This effect results from the irreversibilities induced by the dynamics of the liquid flow. During intrusion, depending on the relative magnitudes of these two thermal effects, the heat observed can be either endo- or exothermic. During expulsion, with both the reversible decrease of the interface and any irreversibilities being exothermic, the integral heat will be exothermic.

Investigated Systems

Three systems have been investigated at 303 K, all consisting of a porous matrix powder plus water enclosed in a polymer membrane. Matrices were selected to have specific characteristics when in contact with water. The first matrix, EVA, was a mesoporous silica gel with organosilanes bearing 8-carbon linear alkyl chains grafted onto the surface, synthesized at the Polytechnic Institute in Kiev.[20,21] Specific surface area was obtained from the nitrogen adsorption/desorbtion isotherms using the BET (Brunauer–Emmett–Teller) method and the porous volume distribution by the BJH (Barrett–Joyner–Halenda) method with the Harkins–Jura equation on desorption branch.[22] The two other matrices, MFI-OH and MFI-F, were

Table 1. Characteristics of the Samples and Energetic Properties of the Systems during Isothermal Compression/Decompression Cycles at 303 K*

Characteristic	Property	System Name		
		EVA + Water	MFI–OH + Water	MFI–F + Water
Characteristics of matrices	Porosity, φ (cm^3/g)	0.51	0.12	0.14
	Pore radius, r_{mean} (nm)	4.0	0.3	0.3
	Specific surface area, Ω (m^2/g)	221	310	400
Characteristics of samples	Powder mass (g)	0.555	0.684	1.032
	Water mass (g)	0.928	1.961	1.806
Mechanical properties	V_{inv} (cm^3/g)	0.43	0.11	0.12
	V_{inv}/φ	86%	92%	88%
	P_{int} (MPa)	21	80	88
	P_{exp} (MPa)	3	76	83
	W_{int}^{Ω} (J/g)	9.2 ± 0.3	5.6 ± 0.6	9.3 ± 0.8
	W_{exp}^{Ω} (J/g)	−1.1 ± 0.3	−5.5 ± 0.6	−8.4 ± 0.8
	$\%W_{degrad}^{\Omega}$	88%	2%	10%
Interfacial heat effect	Q_{int}^{Ω} (J/g)	−6.5 ± 0.2	5.7 ± 0.2	7.5 ± 0.2
	Q_{exp}^{Ω} (J/g)	−1.2 ± 0.2	−5.0 ± 0.2	−7.3 ± 0.2
Interfacial energetic balance	Received energy (J/g)	9.2 ± 0.3	11.3 ± 0.5	16.8 ± 0.6
	Delivered energy (J/g)	−8.8 ± 0.2	−10.5 ± 0.5	−15.7 ± 0.6

*V_{inv} is the invaded volume; W_{degrad} is the fraction of the degraded work.

silicalites, synthesized by the J. Patarin and M. Soulard team at the University of Mulhouse (France). These silicalites are naturally hydrophobic[23,24] and totally microporous, with a structure made of tubes of practically uniform section.[25] The difference between the two matrices comes from their mode of synthesis: a reaction medium containing either OH^- or F^- ions, respectively. Properties and characteristics of the systems are reported in Table 1.

Experimental Studies

All the sample preparations and calorimetric experiments were done at the Laboratoire de Thermodynamique des Solutions et des Polymères, Blaise-Pascal University, Clermont-Ferrand (France).

Materials

Investigation of the heterogeneous systems requires they be placed in small sealed bags that can transmit pressure effects. Small bags made of a thin double-polymer layer (polyethylene/polyamide) membrane were constructed and sealed with an impulse sealer. The geometry (tubelike) of the bag was designed to fit into the measuring cell of the pressure–volume–temperature (*PVT*) calorimeter described hereafter. Both the porous matrix and the liquid must be carefully degassed before coming in contact. For this purpose the special setup shown in Figure 1a was designed.[18] The liquid degassing is done outside the bag by successive solidification/melting cycles with vacuum degassing being done on the frozen solid. A weighed amount of porous material is then introduced into the plastic bag. A tight clamp is used to avoid the powder from being vacuumed up and divides the plastic bag into two compartments. The porous material is roughly degassed under 10^{-2} mbar for 12 h. The degassed liquid is admitted in and forced by a syringe to fill the upper compartment of the bag. After sealing the bag, the separating clamp is removed to allow the solid powder and liquid to come in contact. This manipulation ensures that there is no air in the bag.

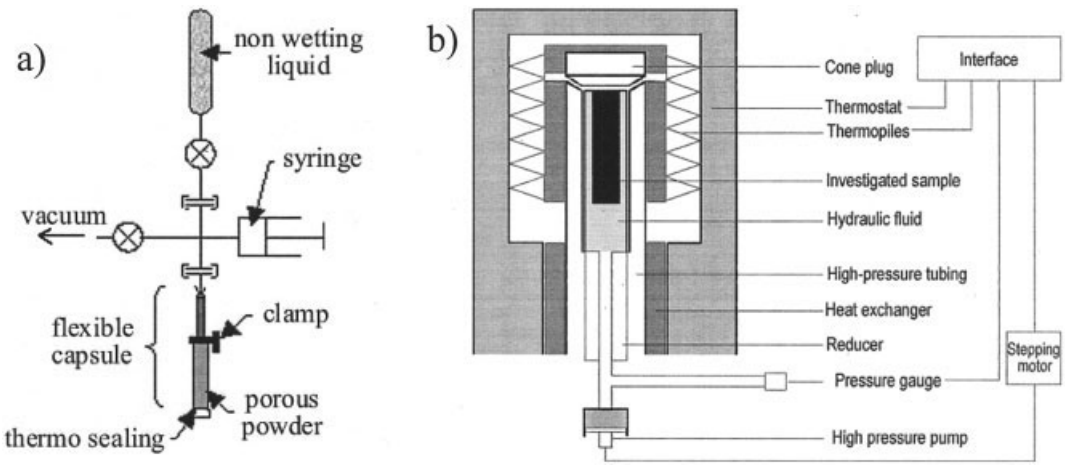

Figure 1. (a) The setup used for degassing and encapsulating the heterogeneous sample; (b) the experimental setup for determining the *PV* diagram and associated heat effects.

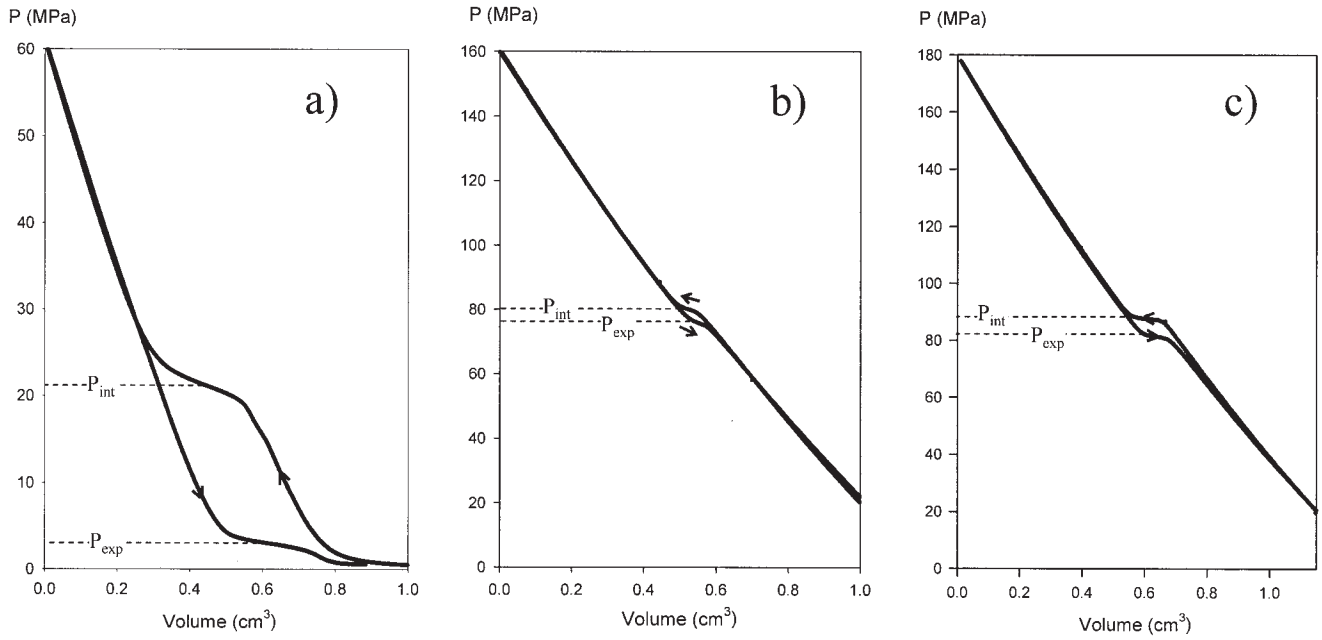

Figure 2. Isothermal (303 K) *PV* diagram during a cycle for (a) EVA + water ; (b) MFI-OH + water; (c) MFI-F + water.

Arrows show the direction of the two curves (compression for the top, decompression for the bottom).

Equipment and procedure

A Setaram C-80 calorimeter, equipped with specially designed high-pressure cells and connected to a high-pressure pump through a hydraulic line, was used for the calorimetric measurements. The experimental technique used in the present work is also known as *scanning transitiometry*.[26,27] The apparatus was designed by S. L. Randzio of the Institute of Physical Chemistry of the Academy of Science in Warsaw, Poland. The *PVT* calorimeter (depicted in Figure 1b) can be operated in different modes. In the present work it was used in the isothermal mode while scanning either pressure or volume. A stepping motor drives the hydraulic pump. By means of a pressure gauge connected to the hydraulic line and of a stepper motor counter, both pressure and volume can be monitored and programmed during scans of one of the two variables (the changes of the dependent variable being recorded). Pressure up to 400 MPa are possible. The calorimeter records the differential heat flow between the measuring cell and the reference cell with a 1 μW detection limit. The volume in the measuring cell was linearly scanned at constant temperature, whereas the pressure change was recorded together with the differential heat flow. Typically, the scanning rate was 10^{-4} cm^3/s; this slow speed was necessary to ensure thermal equilibrium and minimize thermal gradients during the process.

The bag containing the heterogeneous two-phase system is placed in the measuring cell, which is then filled with the hydraulic fluid (mercury) and tightly closed with a special cap. The calorimeter was then lowered over the cells. The close fit of the cells provides good thermal contact between the cells and the thermopiles of the calorimeter. Several cycles of compression followed by decompression were completed at 303 K on each sample. The observed compressibility of the whole system, hydraulic fluid + sample, was corrected by subtracting the hydraulic fluid compressibility measured in blank tests. The measured heat rate was corrected for the heat effects produced by compression/decompression of the hydraulic fluid and the bag through appropriate blank tests.[18]

Results

Isothermal PV diagrams

Figure 2 shows the *PV* diagrams for the three samples. In all three systems the same characteristic pattern is observed. In both compression (top curve) and decompression (bottom curve), practically vertical parallel straight lines, corresponding to the regions of elastic compression of the sample (porous solid + liquid) and two plateaus corresponding to the regions of intrusion and expulsion, respectively, which take place at roughly constant pressures, are observed. The three systems show quite different quantitative mechanical behaviors, however (see Table 1). For the EVA + water system, where matrix pore diameters are larger, intrusion and expulsion take place at relatively low pressures, about 22 MPa, and concomitantly the hysteresis is marked (the decompression curve is noticeably shifted vertically from the compression curve). On the contrary, but in agreement with Eq. 1, the MFI + water systems, which have smaller pores, show intrusion and expulsion at higher pressure (about 80–88 MPa) and concomitantly a smaller hysteresis and thus a quasi-reversible character. The difference of intrusion pressures between the two MFI–water systems was previously observed and described.[12] The presence of fluoride instead of hydroxide anions during the synthesis of MFI-F leads to a porous medium with fewer lattice defects and, consequently, with fewer hydrophilic silanol groups. MFI-F is thus more hydrophobic than MFI-OH. A more hydrophobic material requires higher water intrusion pressures (higher contact angle in Eq. 1), as observed for the MFI-F + water system.

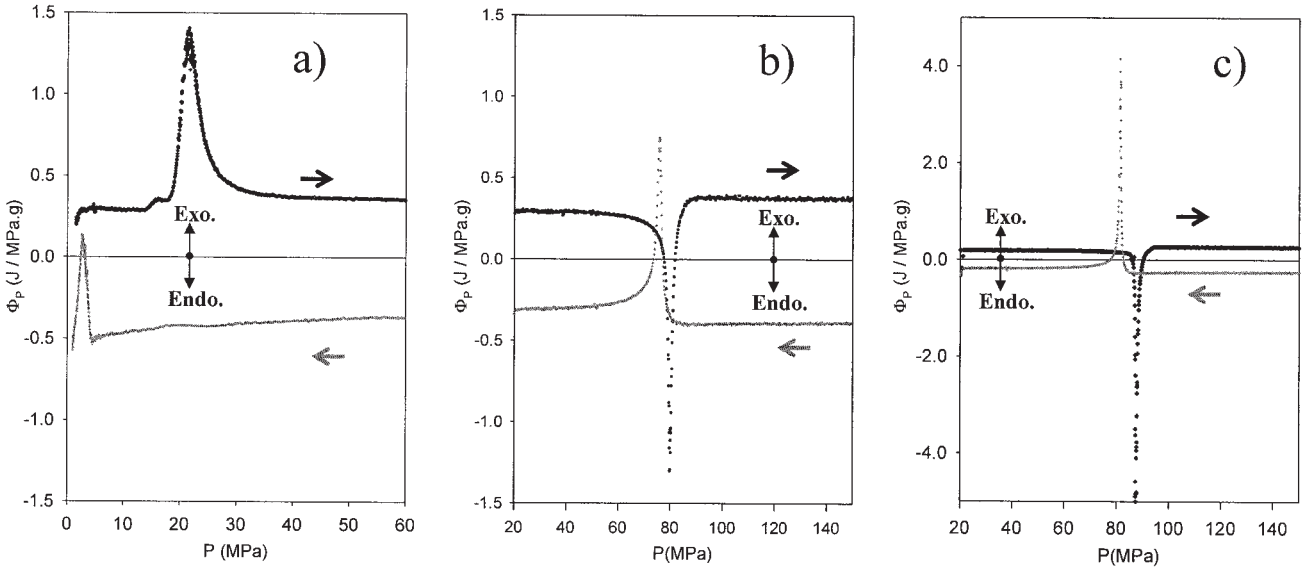

Figure 3. Heat flow Φ_P vs. pressure during a cycle at 303 K for (a) the EVA + water system, (b) the MFI-OH + water system, (c) the MFI-F + water system.

The sign of Φ_P is taken to show exothermic effects upward and endothermic effects downward.

As can be seen Table 1, the porous volume invaded by water during compression is generally close to 90% of the porous volume determined by nitrogen absorption, consistent with what is observed in mercury porosimetry. However, the latter technique is not applicable to MFI because of the narrow pores and to the very high pressures necessary for intrusion. Instead, water porosimetry[28] is more applicable because intrusion pressures are about seven times lower. Table 1 lists the mean values of intrusion and expulsion pressures, that is, the pressures at which the porous volume is filled and drained, respectively, to a maximum.

Table 1 also gives the amount of work produced during intrusion (W_{int}) and during expulsion (W_{exp}). The work degraded during a cycle is given by the (algebraic) sum of these two terms (see Table 1). As expected, this degradation is much larger in the case of the EVA + water systems. Such differences in the mechanical behavior should appear on the thermal behavior as examined below.

Heat effects

The thermograms obtained at 303 K during the first cycle of compression/decompression are shown in Figure 3 for the three systems investigated. The amount of heat generated by each pressure step dQ/dP, Φ_P is shown. The sign of Φ_P is taken arbitrarily positive for exothermic effects and negative for endothermic effects. For each recorded trace, a peak of Φ_P near P_{int} during compression and near P_{exp} during decompression is observed. The base line reflects the heat effects produced by elastic compression or decompression of the bulk liquid and solid. Its value is given by Eq. 9. The baselines for the three samples are approximately the same before and after intrusion or expulsion. As expected, the thermal properties of the solid and the confined liquid after the intrusion or before the expulsion and those of the interface influence the global thermal properties of the system. For the two MFI + water systems, Φ_P is essentially symmetrical on the abscissa, which denotes a high reversibility. The hysteresis shown by the EVA + water system in PV coordinates is corroborated by the heat-effect hysteresis observed in Figure 3a. The broadening of the heat effect during intrusion is explained by the larger pore-size distribution of the EVA matrix. Figure 4 shows for each sample during a compression, the compressibility ε ($\varepsilon = dV/dP$) and the thermal flux Φ_P. There is excellent agreement between the mechanical effects, particularly the ε peaks, and the thermal Φ_P peaks. For MFI–water systems the curves show peaks of the Dirac function type for both Φ_P and ε resulting from the monodispersity of the porous structure.

The main difference between the three systems appears in the heat effect of intrusion. Although intrusion of water into the EVA matrix is exothermic, intrusion of water into MFI matrices is endothermic. The first behavior is now well known[15,16] and, to our knowledge, the second has never previously been described. Equation 18 shows that there is a larger degradation of energy in the EVA system than that in the MFI systems during intrusion.

With respect to the expulsion of water from the three porous solids, the heat effects are exothermic in all cases, which may oppose or even invert the cooling effect of decompression under nonisothermal conditions.

Discussion

Evidence and origin of irreversibilities

After a cycle composed of a compression followed by a decompression, the three systems investigated here return to the same point on the PV diagram. If they are supposed to be purely thermomechanical systems, the total amount of work dissipated during the cycle should be equal to the total amount of heat generated:

$$W_{int} + W_{exp} + Q_{int} + Q_{exp} = 0 \qquad (20)$$

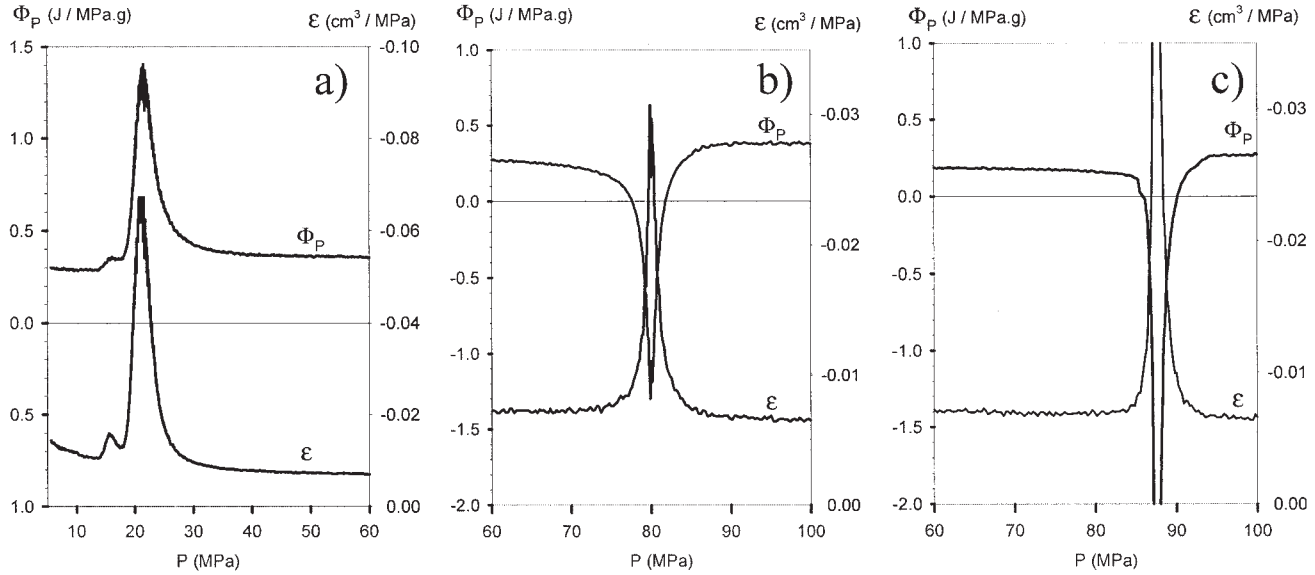

Figure 4. Comparison between the heat flow Φ_P and the compressibility ε as a function of pressure during compression at 303 K for (a) the EVA + water system, (b) the MFI-OH + water system, (c) the MFI-F + water system.

Consequences of the intrusion are distinguishable in both the mechanical and thermal traces.

In another words, by separately considering positive and negative energies—thermal and mechanical—the total amount of energy received by the system must be equal to the total amount of energy delivered during a cycle. In particular, the energetic balance arising from interfacial variations is well satisfied, taking into account the experimental uncertainties for the three systems despite their different characteristics and behaviors, as shown in Table 1.

Concerning the EVA + water system, assuming that the contact angle does not change during intrusion and that the thermomechanical balance was perfectly achieved (the absolute value of $W^{\Omega} + Q^{\Omega}$ should be the same for intrusion and expulsion), a theoretical static contact angle θ_{st}, corresponding to a reversible process, can be estimated with the following equation

$$\cos\,\theta_{St} = -\frac{(W^{\Omega} + Q^{\Omega})_{int}}{\left(\sigma - \mathrm{T}\dfrac{\mathrm{d}\sigma}{\mathrm{dT}}\right)\Omega} \tag{21}$$

Using the surface tension of water σ[29] and the sum of work and heat exchanged during intrusion $(W^{\Omega} + Q^{\Omega})_{int}$, θ_{St} can be compared to the values of the dynamic contact angles θ_R and θ_A computed with the Laplace–Washburn equation (Table 2). The static angle computed for the EVA + water system is quite different from θ_A but very close to θ_R, meaning that intrusion is more irreversible and therefore more exothermic than expulsion. To mechanically initiate intrusion requires more work than initiating expulsion, confirming the fact that intrusion is less spontaneous.

The use of Eqs. 13–16 for MFI + water systems may be questioned, considering the confinement of the liquid in microporous materials with pore size close to the size of the water molecules. At this scale, contact angles have no physical meaning. Moreover, it is likely in these conditions that the surface tension of water is altered[30] and the Laplace–Washburn equation may not be valid for calculating contact angles or pressures of intrusion and expulsion.[24]

Quantitatively, irreversibilities can be estimated for the EVA + water system with Eqs. 17 and 18, the experimentally measured energies, and the computed energies in the theoretical reversible case. In addition, during intrusion and expulsion Eq. 19 can be written

$$Q_{irr,int} = -W_{irr,int} \qquad \text{and} \qquad Q_{irr,exp} = -W_{irr,exp} \tag{22}$$

During intrusion, the results listed in Table 2 for EVA + water system show that the heat generated by irreversibilities counterbalances the endothermic effect expected upon intrusion. Moreover, the irreversibilities would eventually yield a noticeable global exothermic effect. During expulsion, irreversibilities are smaller and the process is close to equilibrium.

Concerning the MFI + water systems, the mechanical results show that irreversibilities must be very small during intrusion as well as during expulsion. However, it remains hard to estimate the irreversibilities effects because, at this pore

Table 2. Reversible and Irreversible Work and Heat Effects Generated during Instrusion and Expulsion in EVA + Water at 303 K

θ_R	θ_{St}	θ_A	W^{Ω}_{rev} (J/g)	Q^{Ω}_{rev} (J/g)	$W_{irr,int}$ (J/g)	$Q_{irr,int}$ (J/g)	$W_{irr,exp}$ (J/g)	$Q_{irr,exp}$ (J/g)
95°	95.8°	128°	1.58	1.08	7.6	−7.5	0.5	−0.1

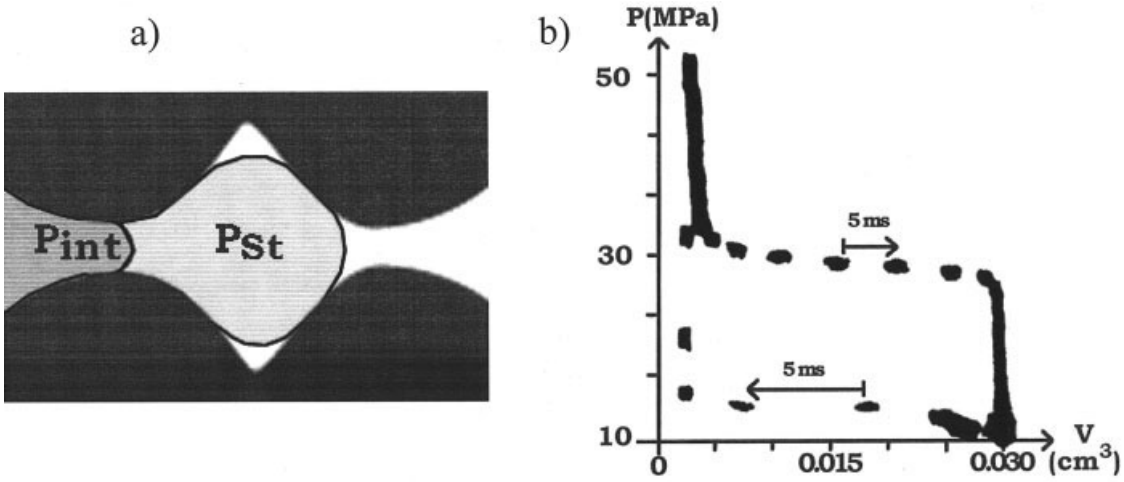

Figure 5. Liquid flow and formation of the interface in an EVA porous geometry type.

(a) Representation of pressures, the intrusion pressure P_{int}, and the static pressure P_{St}, of a liquid flowing in a chamber via a tiny channel; (b) *PV* diagram for a high-speed compression and decompression cycle in the case of a heterogeneous system (from an oscilloscope screenshot).

diameter, Eq. 16 cannot apply quantitatively. In this case, because of low irreversibilities, the intrusion process is logically endothermic and the expulsion process is exothermic within the same order of magnitude (Table 1). Still, irreversibility cannot be nonexistent during both intrusion and expulsion, and probably explains the small differences in the heat effects measured during intrusion and expulsion for these two systems.

Irreversibilities are responsible for the hysteresis observed on the *PV* isotherms because the process degrades mechanical energy into heat. The source is still unknown but the extent of degradation can depend a priori on the history of the state of the surface (hysteresis in the contact angle), on its topology, or on the pore geometry (tortuosity, connectivity).[31] Irreversible viscous dissipation can take place in the bulk liquid when it penetrates or leaves the porous material. However, for a nonwetting flow, the liquid should slip largely over the solid surface.[32,33] Consequently, the velocity profile might be substantially uniform across the flow and the heat generated by viscous flow should be small. The fact that the expulsion process is close to equilibrium supports this argument. Moreover, there are some systems, such as MFI + water, that exhibit very small irreversibilities during intrusion. Viscous dissipation of the liquid flowing into the porous material, at least for these quasi-reversible systems, must be energetically small.

Another source of irreversibility is undoubtedly the structural conformation of the porous surface (superficial roughness[34] and fractal dimension of the surface) or the chemical heterogeneity (grafting and surface faults[35]). Such surface characteristics induce relaxation effects between the liquid and the solid resulting from a variation of the contact angle changing from θ_A to θ_{St} during intrusion and from θ_{St} to θ_R during expulsion. The surface of the EVA matrix, consisting of an agglomeration of particles and grafted with long mobile chains, is particularly complex and modeling, to simulate the liquid flow on this surface, would be quite difficult.

Other factors that contribute to irreversibility could be the rate of intrusion and the consequent kinetic energy. Penetration of water into the porous medium may happen at high speed or by steps (in jerks). The change in the kinetic energy E_C of a water cluster of mass δm_{water} upon acceleration can be expressed as

$$\delta E_C = \beta \frac{\delta m_{water} v^2}{2} \tag{23}$$

where v is the velocity of the water cluster and β is a factor representing the type of liquid flow through the pore. In the present systems where the speed profile is quite constant (plug flow) β is close to 1. The kinetic energy is degraded into heat when the cluster of liquid returns to its resting state; this is an additional type of viscous dissipation. In the case of quasi-static intrusion, the liquid flow could have a high speed but could take place in successive steps. The complex porous architecture of the EVA matrix is the one that dissipates more energy. It is made of convex chambers connected by canals of smaller sizes. Filling a chamber necessitates excess pressure to push the liquid through these restrictions; the liquid arrives in the chamber with a certain velocity followed by a sudden deceleration when it reaches the next restriction. Upon expulsion, the liquid flows out naturally and continuously because the entire porous network has been invaded and the pressure is close to the static pressure (P_{St} in Figure 5a). To quantify this effect we hypothesize that the entire irreversibility expressed as heat (for the EVA + water system) comes from this jerky flow. An estimation of the actual velocity of the liquid in the porous medium during intrusion is given by the following equation

$$v \approx \left(\frac{2|Q_{irr,int}|}{\rho V_{int}} \right)^{1/2} \tag{24}$$

The estimated value exceeds 100 m/s, which is an extremely high value at the microscopic scale; for a porosity of micron size the characteristic time of penetration would be of the order of a nanosecond; thus, this effect cannot solely explain the dissipation. Both volume and surface considerations, taken

together or separately, must be used to explain the energetic dissipation. A systematic study of sufficiently different dissipating systems would be useful to better understand such behavior.

A complementary test on a porous sodium borosilicate glass[36] associated with mercury was made at high speed of compression/decompression at the Kiev Polytechnic Institute, Ukraine. Figure 5b presents a cycle on *PV* coordinates realized in a few hundredths of a second. The points are 5 ms apart, allowing visualization of the speed of intrusion and expulsion, about 30 ms for intrusion and less for expulsion. The result is not of the same order of magnitude as calculated with Eq. 24, but is very small. The velocity of the liquid into pores does not need to be high to permit a very quick operation. Intrusion and expulsion are concerted phenomena among all the pore entries. Only a few millimeters/second for the liquid velocity into the pore is necessary to explain the very small penetration time observed. The more divided the powder, the faster the macroscopic volume variation can be.

Impact of the thermomechanical behavior upon the operation of working lyophobic heterogeneous systems

Data on water indicate a quasi-linear decrease of the surface tension with temperature, expressed with the classical expression[37]

$$\sigma = \sigma_0\left(1 - \frac{T}{T_{cr}}\right)^n \tag{25}$$

For a reversible system the ratio between work and heat exchanged, during intrusion as well as expulsion, can be calculated with Eqs. 13 and 16

$$\frac{W^\Omega}{Q^\Omega} = -\frac{\sigma}{T\dfrac{d\sigma}{dT}} \tag{26}$$

By combining Eqs. 25 and 26, an expression for the exponent n may be obtained, as follows

$$n = \frac{\dfrac{T_{cr}}{T} - 1}{\dfrac{W^\Omega}{Q^\Omega}} \tag{27}$$

For intrusion in the case of the MFI + water systems, which is close to equilibrium (that is, reversible) n values of 0.93 and 1.13 are found for MFI-F + water and MFI-OH + water, respectively. This completely indirect way of estimating the exponent n confirms the quasi-linear dependency of the water surface tension on temperature around 303 K. Thus, Eq. 27 can be simplified in the case of reversible systems involving water to

$$\frac{W^\Omega}{Q^\Omega} \approx \frac{T_{cr}}{T} - 1 \tag{28}$$

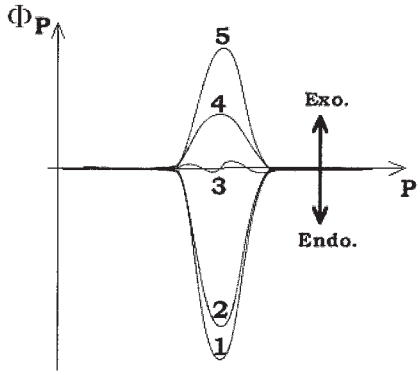

Figure 6. Comparison of the different heat effects (arising from interface formation) measured or expected during intrusion.

1: perfectly reversible (infeasible); 2: like MFI-OH + water; 3: athermic; 4: like EVA + water; 5: completely irreversible.

Now, as has been shown, intrusions can be either exothermic or endothermic, depending on the extent of the hysteresis phenomenon as shown by the *PV* diagrams. As a consequence of the two opposite heat effects—one endothermic and linked to the formation of the interface; the other exothermic, resulting from irreversibility—it is possible for a system to exhibit an athermal intrusion, as illustrated on Figure 6. In this figure Φ_P is an ideal corrected value that represents the heat flow per each pressure step generated by the interface formation during intrusion. To compare the peaks, they were artificially shifted to coincide. Φ_P can vary from endothermic to exothermic, depending on the heterogeneous combination and the irreversibility of the intrusion. For an athermal intrusion, the necessary heat arises solely from the heat produced by the irreversible phenomena and intrusion is then thermally self-generated. Very often, the exchange of heat between the nonwetting liquid and the solid surface is not easily facilitated because of large thermal resistance, named Kapitza resistance,[38] which can constitute a limiting factor for the dynamic intrusion. Then, the advantage of an athermal system is the capacity to respond more rapidly to an interface variation, given that it is in metastable thermal equilibrium. The athermal condition is

$$Q^\Omega_{rev} + Q_{irr,int} = 0 \tag{29}$$

Using Eqs. 3, 13, 16, 22, and 26, and assuming that expulsion is close to equilibrium ($P_{exp} \approx P_{St}$), one can obtain

$$H = \frac{1}{1 - \dfrac{\sigma}{T\dfrac{d\sigma}{dT}}} \tag{30}$$

For systems using water as the nonwetting liquid at 303 K the athermal behavior corresponds to H values close to 0.4, whereas for systems using mercury as the nonwetting liquid athermal behavior corresponds to H values close to 0.1. Because the temperature of investigation is far below the mercury critical temperature, relatively less heat is needed for mercury to develop its surface unit, and even small irreversibilities

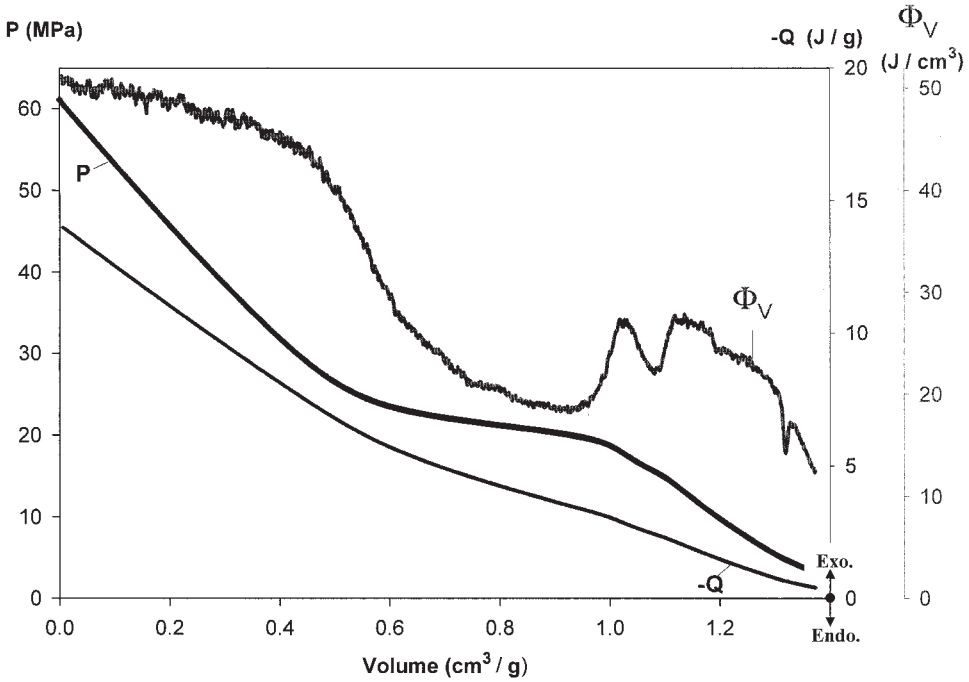

Figure 7. *PV* diagram showing the variation of pressure *P*, the global heat effect $-Q$, and of its derivative Φ_V vs. volume during the compression of EVA + water system at 303 K.

occurring during intrusion easily counterbalance the endothermic effect. This speculated athermal behavior must be confirmed experimentally, but would be an evidence of the coexistence of two antagonist heat effects on intrusion.

To return to the operating mechanical systems, let us consider a simple damper, made of a piston, which contains a heterogeneous lyophobic system such as EVA + water. This system, thanks to its mechanical behavior, can dissipate almost 90% of the work done during a cycle of compression and decompression. For this kind of device, the key variable is not pressure, but the volume of the system delimited by the position of the plunger in the piston pump. In this case, the thermal behavior must be observed as a function of volume. In Figure 7, the pressure, the heat flow per volume increment Φ_V ($\Phi_V = dQ/dV$), and the cumulative heat $-Q$ generated during compression are plotted as a function of the system volume. The Φ_V and $-Q$ curves show that, even if intrusion for this combination is accompanied by an exothermal effect, the effect slows down during intrusion. This relative slowing of the heating is caused by the decrease of the elastic heating of the solid–liquid system (δQ^V in Eq. 5). The elastic heat decrease is induced by the very fast increase in the system compressibility during intrusion, and interface development generates most of the heat. This slowing of the heat generated in the case of the EVA + water system has a positive consequence for operation of this kind of mechanical device because the rise of temperature will be small.

The athermal compression discussed above depends only on interface properties; the bulk volume contribution δQ^V was not considered. In a mechanical device, it must be taken into account and, to achieve global athermal behavior of the device, interfacial development must show a sufficient endothermal effect to balance the heat generated by compression of the bulk components. Coiffard[18] and Eroshenko[17] discussed this possible passage from an interfacial endothermic regime to an interfacial exothermic one through an athermal zone. Figure 8, in which are plotted both the integral heat $-Q$ and the integral work W stored during compression of the MFI-F + water system, outlines this. A mechanical energy storage (W increases) accompanied with an endothermal effect ($-Q$ decreases) occurs with intrusion at about 90 MPa. This endothermal effect tends to balance the naturally exothermal effect arising from compression of the system and an overall athermal zone can be defined from the $-Q$ curve between 50 and 115 MPa. This zone represents the pressure domain for which an athermal mechanical energy storage is possible. For instance, if a piston closes a space filled with MFI-F + water, which is nearly a reversible system, and force is applied so as to make the inner pressure vary between 65 and 100 MPa (see the horizontal line on the $-Q$ curve in Figure 8), then one obtains a working body acting like an athermal "all-or-nothing" spring.

Conclusion

Heterogeneous lyophobic systems made of a porous, solid matrix suspended in a nonwetting liquid can be used as mechanical devices to store, dissipate, or transform mechanical energy. By a microcalorimetric study of their behavior during isothermal compression/decompression cycles it was shown that such devices are globally thermomechanical systems. The thermal response to an external compression occurs in a zigzag manner: heat production resulting from compression of the whole system, absorption of heat during intrusion (which can be partially counterbalanced by exothermic irreversible phenomena), and finally another exothermic effect (after completion of the invasion of the porous volume). The thermal evo-

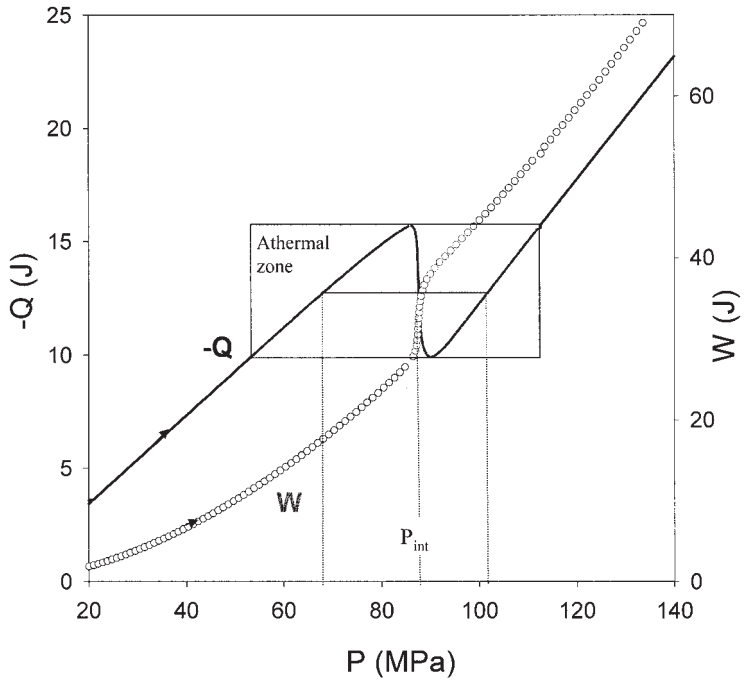

Figure 8. Thermal ($-Q$) and mechanical (W) energies vs. pressure during the compression of the MFI-F + water system at 303 K.

The athermal zone represents the zone wherein an athermal compression (horizontal line on the $-Q$ curve) is possible taking two limiting working pressures in the range 50–85 MPa for the bottom one and in the range 90–115 MPa for the top one.

lution during spontaneous decompression always takes place in a zigzag manner: two ascending branches of heat absorption arising from expansion of the bulk liquid and solid either invaded or not and, in between, a descending branch attributed to the always exothermal expulsion.

A thorough investigation of the thermomechanical behavior of heterogeneous systems of different geometries, topologies, and porous surfaces provides better understanding of and quantifies possible irreversibilities occurring during intrusion and expulsion. Small-size pores together with narrow size distribution and simple topology, as in the case of microporous naturally hydrophobic MFI silicalites, ensure a continuous formation of the solid–liquid interface during intrusion. At constant pressure a quasi-reversible storage of work and heat is observed. On the contrary, larger-size pores and connecting canals as well as complex topology and porous surface, as in the case of functionalized silica gels (grafted with organic chain molecules), impose a jerky intrusion. This intrusion is marked by a nonreversible formation of the solid–liquid interface. Consequently, under isothermal conditions an induced exothermic effect may counterbalance, more or less completely, the endothermic creation of the interface. In the case of the EVA + water system studied here, the overall effect is exothermic.

Between the reversible endothermic intrusion regime and the irreversible exothermic regime, an athermal regime theoretically exists for which all the mechanical energy is entirely degraded and used in situ to form the solid–liquid interface. As a matter of fact, a thermally self-regulated regime of intrusion may be possible. Considering the problems of controlling temperature in such systems, often confined in closed spaces, this kind of athermal working system is of greatest interest, particularly for applications necessitating high-frequency cycles. Another interesting conclusion is evidently the possible use of such systems to dissipate mechanical energy without notable heat generation.

Finally, it should be understood that the present thermomechanical investigation did not take into consideration other possible sources of energy transformation (radiation, sound, electricity, etc.), which could influence the overall energy balance. So far, we believe that their contribution is marginal within the present experimental uncertainties. However, the electromagnetic compatibility of operational systems based on variations of a repulsive solid–liquid interface would be worth future investigation.

Acknowledgments

This work was supported by the Délégation Générale pour l'Armement (DGA), (marché n° 99 22 207) within the DUAL joint research program between DGA and CNRS in France (IGA). A. Quenzer (DGA) and C. Petiau (Dassault Aviation) are gratefully acknowledged for their contribution. We thank S. Tkatshenko (Kiev Polytechnic Institute, Ukraine) for technical assistance in high-speed tests, and Prof. L. D. Hansen (Brigham Young University, Provo, UT) for reading and improving the manuscript.

Notation

E_c = kinetic energy, J
Endo. = endothermic direction
Exo. = exothermic direction
H = hysteresis coefficient
m = mass, kg
n = coefficient of linearity
P = pressure, MPa
Q = thermal energy, thermal energy per gram of solid, J, J/g
r = pore radius, m
S = entropy, J/K
S_c = entropy production, J/K

T = temperature, K
T_{cr} = critical temperature, K
U = internal energy, internal energy per gram of solid, J, J/g
v = speed of liquid clusters
V = volume, volume per gram of solid, m^3, cm^3/g
W = work, work per gram of solid, J, J/g

Greek letters

α_P = isobaric thermal expansivity, 1/K
β = kinetic energy coefficient
ε = volume variation per pressure variation, cm^3/MPa
Φ_P = heat flow per pressure variation and gram of solid, J/MPa.g
Φ_V = heat flow per volume variation, J/cm^3
φ = porosity, cm^3/g
κ_T = isothermal compressibility, 1/MPa
θ_A = advancing contact angle, °
θ_R = receding contact angle, °
θ_{St} = static contact angle, °
ρ = density, kg/m^3
σ = surface tension of the liquid, N/m
σ_0 = surface tension of the liquid at 0 K, N/m
Ω = specific surface, surface of developed interface, m^2/g

Subscripts

exp = expulsion of the liquid from the invaded porosity
int = intrusion of the liquid into the empty open porosity
irr = irreversibility of the transformation
inv = penetration of the liquid into the matrix
rev = reversible transformation

Superscripts

L = bulk liquid
M = solid skeleton (matrix)
V = bulk volume (liquid + matrix) without interface
Ω = solid–liquid interface

Literature Cited

1. Eroshenko VA. Thermodynamics of intrusion of liquid metals into solid porous matrices. *The Properties of Capillarity and Adhesion of Melts* (in Russian). Science Academy of Ukraine, Kiev: Naukova Dumka; 1987;100-109.
2. Eroshenko VA. The unexpected properties of a complex thermodynamical system (in Russian). *C R Sci Acad Ukr A.* 1990;10:79-82.
3. Eroshenko VA. *The Characteristic and Unexpected Properties of a Complex Thermodynamical System* (in French). Nancy, France: Actes JETC4; 1995:379-397.
4. Eroshenko VA. Space dimensionality as thermodynamic potential of a system (in French). *Entropie*. 1997;202/203:110-114.
5. Eroshenko VA. Eroshenko hydrocapillary accumulator. Patent Number 1333870, URSS (priority of 24.05.1985)—Russia; 1993.
6. Eroshenko VA. Hydrocapillary accumulator. Patent Number 943444, URSS (priority of 28.04.1980)—Russia; 1993.
7. Eroshenko VA. Heterogeneous structure for accumulation or dissipation of energy, process to use it and associated devices. Int. Patent WO 96/18040; 1996.
8. Eroshenko VA. Eroshenko rotating thermal engine. Patent Number 1452262, URSS (priority of 16.06.1986)—Russia; 1993.
9. Eroshenko VA. Heterogeneous thermodynamical system, thermodynamical cycle and device for turning heat into work. Patent Number 1382078, URSS (priority of 20.01.1982)—Russia; 1993.
10. Eroshenko VA. High dissipating damper. Int. Patent WO 55 2001; 616:1-33.
11. Suciu CV, Iwatsubo T, Deki S. Investigation of a colloidal damper. *J Colloid Interface Sci.* 2003;259:62-80.
12. Eroshenko VA, Regis R-C, Soulard M, Patarin J. Energetics: A new field of applications for hydrophobic zeolites. *J Am Chem Soc.* 2001; 123:8129-8130.
13. Laouir A, Luo L, Tondeur D, Cachot T, Le Goff P. Thermal machines based on surface energy of wetting: Thermodynamics analysis. *AIChE J.* 2003;49:764-781.
14. Eroshenko VA. Effect of heat exchange on filling of lyophobic pores and capillaries with liquid. *Colloid J.* 1987;49:769-773.
15. Gusev VY. On thermodynamics of permanent hysteresis in capillary lyophobic systems and interface charaterization. *Langmuir.* 1994;10: 235-240.
16. Gomez F, Denoyel R, Rouquerol J. Determining the contact angle of a nonwetting liquid in pores by liquid intrusion calorimetry. *Langmuir.* 2000;16:4374-4379.
17. Eroshenko VA. Exo and endo effects during progressive compression in lyophobic heterogeneous nanosystems. Private communication.
18. Coiffard L. *Study of Lyophobic Heterogeneous Systems "Porous Matrix–Liquid." An Insight into the Nature of Hysteresis in Isothermal Compression/Decompression Processes Using Scanning Transitiometry* (in French). PhD Thesis D.U. 1303. Clermont-Ferrand, France: Université Blaise-Pascal; 2001.
19. Eroshenko VA. Influence of the specific interface in a lyophobic heterogeneous system upon observable thermal effects during the isothermal compression of the system. *Ross Khim J.* (*D.I. Mendeleev*). 2002;46:31-38.
20. Eroshenko VA, Fadeev AYu. Intrusion and expulsion of water in hydrophobized porous silica. *Colloid J.* 1995;57:446-449.
21. Fadeev AY, Eroshenko VA. Study of penetration of water into hydrophobized porous silica. *J Colloid Interface Sci.* 1997;187:275-282.
22. Gregg SJ, Sing KSW. *Adsorption, Surface Area and Porosity*. 2nd ed. London: Academic Press; 1982.
23. Flanigen EM, Bennett JM, Grose RW, Cohen JP, Patton RL, Korchner RM, Smith JV. Silicalite, a new hydrophobic crystalline silica molecular sieve. *Nature.* 1978;271:512-516.
24. Eroshenko VA, Regis R-C, Soulard M, Patarin J. The heterogeneous systems 'water–hydrophobic zeolites': New molecular springs (in French). *C R Acad Sci France, Phys.* 2002;3:111-119.
25. Meier M, Olson DH, Baerlocher C. Atlas of zeolite structure types. *Zeolites.* 1996;17:1-230.
26. Randzio SL. Scanning transitiometry. *Chem Soc Rev.* 1996;25:383-392.
27. Randzio SL, Grolier J-PE. Supercritical transitiometry of polymers. *Anal Chem.* 1998;70:2327-2330.
28. Eroshenko VA, Fadeev AYu. Water porosimetry for hydrophobic porous materials investigation (in Russian). *Ross Khim J.* (*D.I. Mendeleev*). 1996;XL:92-99.
29. IAPWS Release on Surface Tension of Ordinary Water Substance, The International Association for the Properties of Water and Steam, September; 1994.
30. Buffey IP, Brown WB, Gebbie HA. A theoretical study of the infrared absorption spectra of large water clusters. *J Chem Soc Faraday Trans.* 1990;86:2357-2360.
31. Eroshenko VA. Private communication, DGA-ENSTA, Paris, France, June 27; 1996.
32. Vinogradova OI. Slippage of water over hydrophobic surfaces. *Int J Miner Process.* 1999;56:31-60.
33. de Gennes PG. On fluid/wall slippage. *Langmuir.* 2002;18:3413-3414.
34. Wenzel RN. Resistance of solid surfaces to wetting by water. *Ind Eng Chem.* 1936;28:988.
35. Miller CA, Neogi P. *Interfacial Phenomena*. New York, NY: Marcel Dekker; 1985.
36. Venzel BI, Svatoskaya LG. Structure of porous glasses and the possibility of their variation control. *Opt Appl.* 1994;24:1-2.
37. Van-der-Waals JD, Kohnstamm Ph. *Lehrbuch der Thermostatic*. Leipzig, Germany: Verla von Johan Ambrosius Barth; 1927.
38. Barrat JL, Bocquet L. Large slip effect at a non-wetting fluid-solid interface. *Phys Rev Lett.* 1999;82:4671-4674.

Manuscript received Apr. 11, 2003, and revision received July 30, 2004.